Journal of
Materials Chemistry B

Materials for biology and medicine

Accepted Manuscript

This article can be cited before page numbers have been issued, to do this please use: M. Barbalinardo, M. di Giosia, I. Polishchuk, G. Magnabosco, S. Fermani, F. Biscarini, M. Calvaresi, F. Zerbetto, G. Pellegrini, G. Falini, B. Pokroy and F. Valle, *J. Mater. Chem. B*, 2019, DOI: 10.1039/C9TB01148J.

ROYAL SOCIETY OF CHEMISTRY

rsc.li/materials-b

View Article Online
DOI: 10.1039/C9TB01148J

ARTICLE

Received 00th January 20xx,

Accepted 00th January 20xx

DOI: 10.1039/x0xx00000x

Retinoic acid/calcite micro-carriers inserted in fibrin scaffolds modulate neuronal cell differentiation

Marianna Barbalinardo[a†], Matteo Di Giosia[b†], Iryna Polishchuk[c] , Giulia Magnabosco[b], Simona Fermani[b], Fabio Biscarini[d], Matteo Calvaresi[b], Francesco Zerbetto[b], Graziella Pellegrini[e,f], Giuseppe Falini[b]*, Boaz Pokroy[b] , Francesco Valle[a,g]*

The controlled release of cell differentiating agents is crucial in many aspects of regenerative medicine. Here we propose the use of hybrid calcite single crystals as micro-carriers for the controlled and localized release of retinoic acid which is entrapped within the crystalline lattice. The release of retinoic acid occurs only in the proximity of stem cells, upon dissolution of the calcite hybrid crystals that are dispersed in the fibrin scaffold. These hybrid crystals, provide a sustained dosage of the entrapped agent. The environment provided by this composite scaffold enables differentiation towards neuronal cells that form a three-dimensional neuronal network.

Introduction

Efficient modulation of cell differentiation requires spatiotemporal control of the release of differentiating agents. This can be obtained by embedding an active molecule in a slow controlled-release system, localized within the scaffold that hosts the cells.[1, 2]

Calcite, the thermodynamically most stable polymorph of calcium carbonate, can be used as a delivery system for active molecules due to its ability of (i) embedding molecules within its crystalline lattice forming hybrid crystals, and (ii) selectively releasing them only upon dissolution, which occurs at acidic pHs, such as those typical of inflamed and cancer tissues. These hybrid crystals enable modulation and localization of the release and provide a sustained dosage of the entrapped agents over an extended period of time, instead of an initial burst-like release.

The capability of calcite to host various molecules and macromolecules within its crystalline lattice was discovered in biominerals. Berman et al. demonstrated that glycoproteins were entrapped within magnesium calcite single crystals (about 0.3 wt.%) that form sea urchin spines, increasing their resistance to breakage and cleavage.[3] After that finding, the entrapment of macromolecules within crystalline lattice has been observed in almost every biomineral.[4-7] It has been shown, that the incorporated organic molecules always lead to lattice distortions that can be detected via synchrotron High Resolution Powder X-ray Diffraction (HRPXRD)[8, 9].

In parallel, inspired by nature, much effort has been made toward the production of hybrid single crystals embedding various types of single molecules and molecular assemblies in order to obtain novel functional materials.[7, 9-12] Among many case studies, it is worth mentioning doxorubicin/calcite single crystals that were synthesized and provided a controlled release system for cancer cell treatment.[13] Doxorubicin was uniformly embedded within the calcite crystals and slowly released, only in the proximity of the targeted cancer cells.

In a technological perspective, intrinsically colorless and diamagnetic calcite single crystals were turned into colored and paramagnetic solids through the incorporation of Au and Fe_3O_4 nanoparticles without significantly disrupting the crystalline lattice of calcite.[14, 15] Sulfonated fluorescent dyes characterized by different emission wavelengths were successfully occluded within calcite lattice and white emission was obtained by precipitation in the presence of the proper ratio of different dyes.[16] Apart from obtaining a white emitting device, inclusion of dyes in calcite lattice allows simplicity of a) dye localization and b) study of the mechanism of their interaction with the growing surface.

Perlucin, a recombinant biomineralization protein, fused to green fluorescent protein was incorporated into the calcite structure and induced concentration-dependent anisotropic lattice distortions along the host's c-axis very similar to those observed in biominerals .[17] Larger systems, such as micelles[18-20] and block co-polymers have been occluded within calcite single crystals and it was assessed that

[a.] *Consiglio Nazionale delle Ricerche (CNR), Istituto per lo Studio dei Materiali Nanostrutturati (ISMN), Via P. Gobetti 101, 40129 Bologna, Italy.*
[b.] *Dipartimento di Chimica "Giacomo Ciamician", Alma Mater Studiorum - Università di Bologna, via F. Selmi 2, 40126 Bologna, Italy.*
[c.] *Department of Material Sciences and Engineering and the Russel Berrie Nanotechnology Institute Technion-Israel Institute of Technology, 32000 Haifa, Israel.*
[d.] *Dipartimento di Scienze della vita, Università di Modena e Reggio Emilia, Via Campi 103, 41125 Modena, Italy.*
[e.] *Center for Regenerative Medicine ''Stefano Ferrari'', University of Modena and Reggio Emilia, Modena, Italy*
[f.] *Holostem Terapie Avanzate, Modena, Italy*
[g.] *Consorzio Interuniversitario per lo Sviluppo dei Sistemi a Grande Interfase (CSGI), ISMN-CNR, 40129 Bologna, Italy;*
† These authors contributed equal.
Corresponding Author
* Francesco Valle - E-mail: francesco.valle@cnr.it
* Giuseppe Falini - E-mail: giuseppe.falini@unibo.it

Electronic Supplementary Information (ESI) available: [details of any supplementary information available should be included here]. See DOI: 10.1039/x0xx00000x

the formation of a single crystal composite enhances mechanical proprieties of the calcite host, similarly to what observed in nacre.[21] In all these cases as well as when single amino acids are incorporated, lattice distortions are detected[22]. Hence, it is well accepted to date, that lattice distortions that relax upon heat treatments are a finger print of incorporated organic molecules.

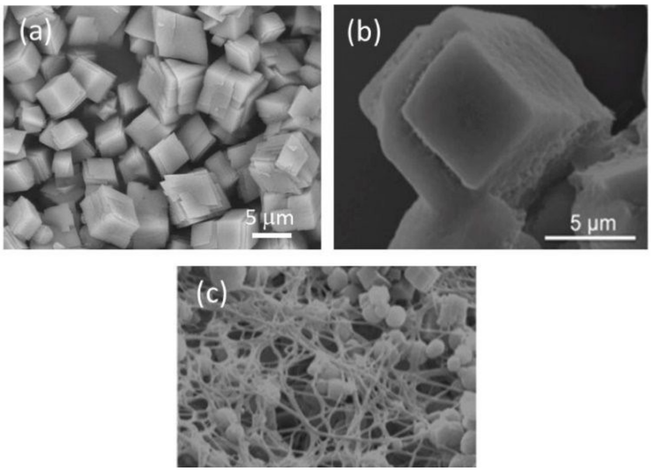

Figure 1 SEM images of a) calcite crystals, b) calcite crystals grown in the presence of 200 µM RA and c) the same crystals are occluded within the fibrin structure

Because of the ascertained and remarkable ability of calcite to act as a host matrix for various water dispersed species, the present work has been devoted to: (*i*) describe for the first time the synthesis of calcite crystals entrapping retinoic acid (RA), and (*ii*) report the inclusion of these composite crystals into fabricated bioactive fibrin scaffolds in order to control the release of RA for inducing differentiation of the cells.[23]

The main advantage of using this system compared to direct incorporation of RA in the fibrin scaffold is that the calcite micro-carriers avoid a single burst release because of the slow, pH dependent dissolution of the $CaCO_3$ crystals, which effectively enables fine-tuning and triggering of the release towards cells.

The hybrid system is completely biocompatible and biodegradable since $CaCO_3$ dissolves into calcium and carbonate ions, which can be easily eliminated by the organism. Furthermore, this system provides an extended release in the case of an implanted device, thus avoiding the need of sequential drug administrations.

Results and discussion

In order to verify the possibility of using single crystals of calcite as micro-carriers of molecules able to regulate cell growth processes, RA was used as differentiation factor of stem cells, while fibrin was used as bioactive scaffold. RA is a potent metabolite of vitamin A and acts as a growth and differentiation factor in many tissues.[24, 25] Fibrin is commonly used as a biological scaffold for stem or primary cells to regenerate adipose tissue, bone, cardiac tissue, cartilage, liver, nervous tissue, ocular tissue, skin, tendons and ligaments.[26-32] In the present study, neuroectodermal stem cells (NE-4C) and human neuroblastoma cells (SH-SY5Y) were used, in minimal essential medium, to test if the delivery of RA from the calcite carriers can induce their differentiation.

Calcite crystals were grown in the presence of a 200 µM RA solution. In this condition, solely calcite crystals formed. The hybrid systems were surface cleaned of RA. The SEM images reported in figure 1 do not show relevant morphological differences between pure calcite crystals and those grown in the presence of 200 µM RA. RA/calcite hybrid single crystals show the typical {104} faces and have a uniform size distribution of 5 µm along the c-axis. These crystals had a loading of 0.12 wt. % of RA. The cell differentiation results obtained using the surface cleaned RA-entrapping crystals are in agreement with a progressive release of RA upon crystal dissolution. In fact, as shown in figure 2 and figure S1, RA is released upon dissolution of the calcite/RA hybrid crystals, with an increased released at the slightly acidic environment typical of the proximity of these cell lines. [33]

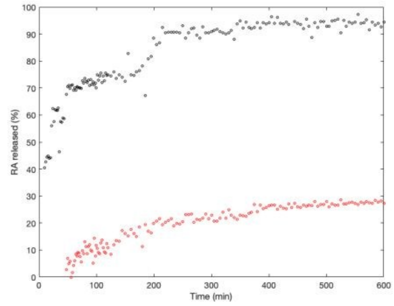

Figure 2 Kinetic of release of RA by calcite/RA hybrid crystals in PBS pH 7.4 (red) and citrate buffer pH 6.2 (black) estimated by measuring the UV-Vis absorbance at 290 nm.

The incorporation of RA into the calcite lattice has been investigated by synchrotron HRPXRD. Rietveld refinement of collected diffraction patterns shows that the inclusion of RA into calcite structure causes lattice strain of 7.62E-05 along the c-axis and of 3.53E-05 along the a-axis, compared to pure calcite crystals.

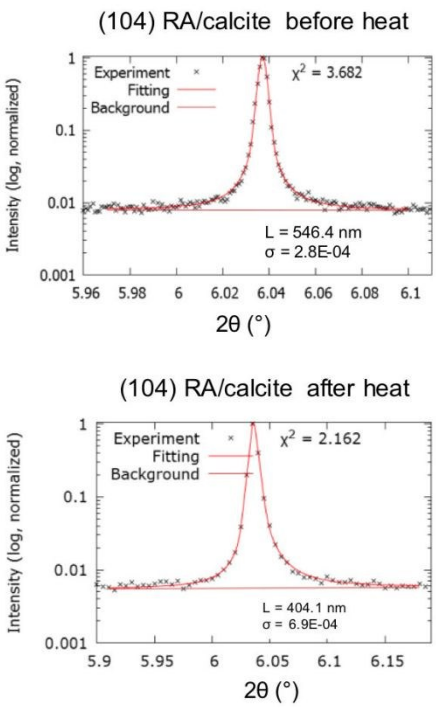

Figure 3 . Line profile analysis of the (104) calcite diffraction peak collected from calcite crystals grown in the presence of 200 µM RA before (left) and after thermal treatment (right), where L is crystallite size, σ– microstrain fluctuations and x^2 – goodness of fit

View Article Online
DOI: 10.1039/C9TB01148J

Not only was the strain relaxed after a thermal treatment at 250 °C for 180 min, but moreover, we also observed broadening of the post-annealed diffraction peaks. We performed line profile analysis of the (104) diffraction peak collected from the crystals containing RA before and after annealing (Fig. 3). After annealing, the crystallite size decreases, while microstrain fluctuations increase, as compared to those prior to heat treatments. This latter observation is common for the behavior of composite bio-crystals upon annealing[34] and demonstrates unequivocally that the RA is located within the crystalline lattice of the calcite.

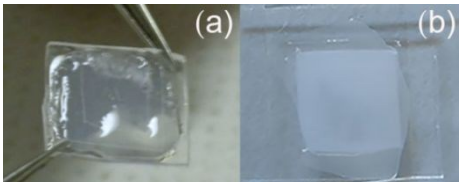

Figure 4 Fibrin. (a) without and (b) with RA/calcite hybrid single crystals

The combination of RA/calcite hybrid single crystals with fibrinogen and thrombin yielded a gel slightly less transparent than that made of pure fibrin, due to the light scattered by the embedded particles (figure 4). SEM microscope image (figure 1c) illustrates the homogeneous inclusion of the micro-carriers within the fibrin fibrous matrix.

The differentiation of NE-4C/SH-SY5Y cells into a densely interconnected neuronal network was first assessed seeding the cells in the presence of the RA/calcite hybrid single crystals, figures 5a, b. This step demonstrates that the micro-carriers loaded with RA are able to induce differentiation by locally releasing the active molecule to the cells. This effect is due to the slow etching of the crystals in the slightly acidic environment in the proximity of these cell lines.[33] When the same experiment was carried out with pure calcite, no differentiation took place and the crystals displayed almost no toxicity (figure 5c, d).

A progressive morphological change of the cells was observed during the differentiation process. After prolonged time of incubation (from day 5) neuronal processes become visible and the active areas are almost completely covered by a dense layer of mature neuronal cells. Figures 5a and b show typical fluorescence microscopy results of the neuronal network at eight days upon induced differentiation (day 8) after co-staining with specific probes. This clearly demonstrates the presence of differentiation of the majority of cells and the formation of a dense neuronal network with long and interconnected neuronal filaments. The images show that there is also a substantial growth of the network in the presence of RA-loaded microcrystals.

The differentiation of the cells in the RA/calcite-fibrin composite was monitored following the same protocol. It is worth underlying that this is a 3D scaffold fully biodegradable and bioresorbable.

The images displayed in figure 6 were obtained at the end of the differentiation, NE-4C cell successfully differentiated on the scaffold as proved by the immunofluorescence staining. Optical and SEM micrographs revealed that the neurite processes are still attached to the area of the microcrystal, indicating that the calcium present both in the crystals and in the fibrin does not negatively affect cell viability and neuronal maturation.

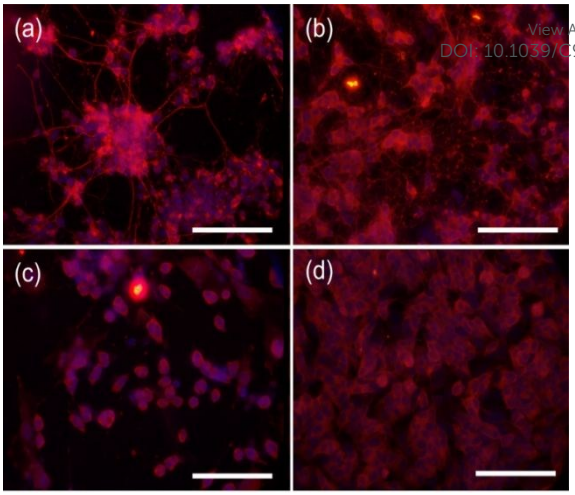

Figure 5 Immunofluorence images. The red color (III β-tubulin) marks the microtubule and the neuronal filament. Scale bars are 100μm. (a and b) Cell differentiation at day 8 by retinoic acid released from the fibrin-calcite/RA hybrid single crystals; (a) formation of the neuronal network of NE-4C in astrocytes, (b) differentiation of SH-SY5Y cells into neurons. The blue color (DAPI) marks the nuclei of the cells. The differentiation is visualized by the specific labelling of III β-tubulin, a typical marker of neuronal processes (red). Control experiments are reported in (c) and (d) cells after 8 days of incubation in the composite fibrin/calcite crystals without retinoic acid; (c) NE-4C cells, (d) SH-SY5Y cells; the network is not present and III β-tubulin is not localized in any filament.

To confirm the result obtained by the release of RA by means of the calcite crystals, we carried out control tests on pure fibrin and on fibrin-bare calcite. Figures S2 and S3 respectively show the results obtained by differentiating the cells on a simple fibrin gel and on the fibrin with unloaded calcite where the RA was supplied in solution. There are not differences compared to the results obtained by incorporating RA in crystals, thus confirming the retention of the proprieties of RA even after the release from the crystals. Figures 5 (c and d) show that within the fibrin with crystals without RA both cell lines continue to proliferate but no differentiation is visible.

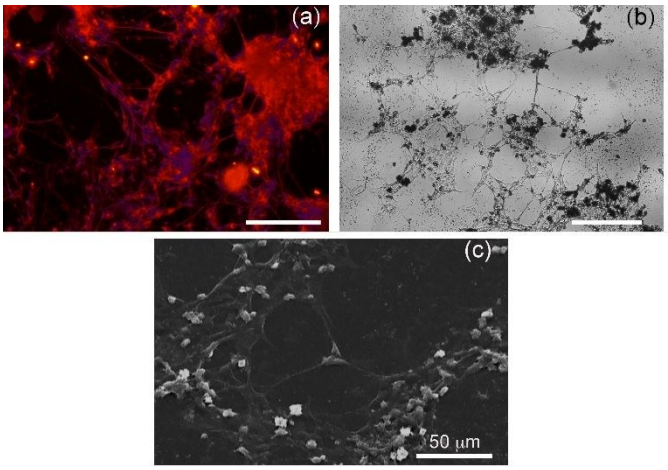

Figure 6 NE-4C cell differentiation day 8 through fibrin-calcite/RA hybrid crystals. Immunofluorescence images: (a) optical images: (b) SEM images: (c) the formation of the neuronal network of NE-4C in astrocytes. Scale bars are 100μm.

Experimental

Synthesis of RA/calcite hybrid crystals

Calcite crystals were synthesized by dropwise addition of 2 ml of 500 mM Na_2CO_3 to a solution containing 2 ml of 500 mM $CaCl_2$ and 1 ml of 1 mM RA under vigorous stirring. After 24 hours the crystals were collected by filtration under vacuum using a RC 0.45 µm filter (Sartorius), thoroughly washed with distilled water and ethanol, and then air-dried. The solution in which the crystallization occurred was kept for quantification of the residual RA.

Calcite crystals for High-Resolution X-Ray Powder Diffraction (HRXRPD) have been synthesized using the vapor diffusion method. Briefly, ammonia and CO_2 obtained from decomposition of solid $(NH_4)_2CO_3$ were allowed to diffuse in 750 µL of a solution containing 10 mM $CaCl_2$ and 200 µM RA in a closed desiccator. The crystallization process was allowed to proceed for 4 day, after which the crystals were washed 3 times with distilled water, once with ethanol and air-dried.

RA quantification

RA content in the produced crystals was evaluated by UV-Vis spectroscopy measuring the intensity of the RA absorption band at 290 nm. Briefly, the residual RA was quantified after the precipitation process and the RA wt.% was calculated as the ratio between RA and the calcium carbonate obtained during the synthesis. RA calibration curve was obtained using the standard addition method to consider the matrix effect due to the Ca^{2+} still present in the solution.

Fabrication of micro-carriers with retinoic acid

The composite material was prepared by first combining fibrinogen (10 mg/ml) with thrombin (0.5 NIH unit corresponding to 0.065 µg/ml) to achieve the fibrin network formation, then the microcrystals were added to the reticulating fibrin to get a full incorporation.

For the experiments where only the micro-carriers were present, calcite microcrystals were drop casted onto glass slides where cell lines were then seeded.

β-Tubulin III Antibody Staining

Tubulins are the major components of cellular cytoskeleton, class III β-tubulin is a microtubule element expressed exclusively in neurons and is a popular marker specific for this kind of cells and thus to assess a proper differentiation towards these lines.[35i] The detailed steps of the staining protocol are: cultured cells are fixed with 4% paraformaldehyde in 1X PBS for 15-20 minutes at room temperature; they are then washed twice with 1X washing buffer. To permeabilize cells 0.1% Triton X-100 in 1X PBS is added for 1-5 minutes at room temperature and then washed twice with 1X washing buffer. Blocking solution (BSA) and primary antibody (Anti-β-Tubulin III) in blocking solution are applied for 30 minutes and 1 hour respectively at room temperature and then washed three times (5-10 minutes each) with 1X wash buffer. Secondary antibody (Alexa fluor 594) freshly diluted in 1X PBS is incubate for 30-60 minutes at room temperature and washed three times with 1X washing buffer. Following this washing step, nuclei counterstaining can be performed by incubating cells with DAPI (4',6-diamidino-2-phenylindole) for 1-5 minutes at room temperature, followed by washing cells three times (5-10 minutes each) with 1X washing buffer[36]. Fluorescence images have then been collected with a fluorescence microscope Nikon Eclipse I80, equipped with appropriate fluorescence filters and a Nis-Elements F300 CCD camera.

Scanning electron microscopy observations

The composite material fibrin-microcrystals was characterized by scanning electron microscopy (SEM) imaging. The images were collected using a Hitachi S4000 FEG-SEM. Samples had to undergo a preparation typical of biological materials[37]: 2.5% gluteraldehyde in phosphate buffered saline (PBS) buffer was added at 4 °C for 1 hour. Each sample was then rinsed three times in PBS for 5 minutes before being incubated for 1 hour with 1% osmium tetra-oxide (OsO_4). The samples were then rinsed 3 times with distilled water 10 minutes each time. A sequential dehydration in 50%, 75%, 95% and 99% ethanol was then performed before coating the sample surface with a 10 nm thick gold layer by sputtering.

High resolution X-ray powder diffraction measurements

High resolution X-Ray powder diffractogram were collected at European Synchrotron Radiation Facility (Grenoble, France), beamline ID22, using a wavelength of 0.4959 Å. Diffraction patterns were converted to Cu Kα wavelength (1.5406 Å) for easier understanding.

Kinetic of release

The kinetic of release of RA from calcite crystals has been studied by measuring the RA released during dissolution via UV-Vis spectroscopy (Agilent Cary-60). In a typical experiment, 5 mg of RA/calcite hybrid crystals have been added to 800 µL of buffer and the absorbance spectra have been recorded for 10 hours. The buffer used are 1 M citrate buffer at pH 6.2 to simulate the surrounding of the cells and PBS buffer at pH 7.4 to simulate areas distant from the cells. The data have been normalized on the maximum amount of RA released after 10 hours.

Cell culture and differentiation

Two cell lines were used in this work: NE-4C and SH-SY5Y. 25,000 cells per cm^2 were seeded as required by the differentiation protocol[38]; after 4 hours from sowing, the time required for cell adhesion, differentiation was induced by replacing the medium with differentiation medium composed of DMEM F-12 Ham (1:1), 1X insulin/transferrin/selenium (ITS), 4 mM glutamine, 40 µg ml^{-1} gentamicin and 2.5 µg ml^{-1} amphotericin (DM); 1µM all-trans retinoic acid (RA) was present only in the control experiments. After two days, the DM was replaced by DM containing 40 ng ml^{-1} neurothropic brain-derived factor (BDNF). Half of the DM was then changed every day by subsequent replacing it with DM, without any inducers until the end of the experiment. Cell-free reference devices were subjected to the same protocol without the initial cell seeding. As a control, the same differentiation protocol was applied in parallel also to cells seeded on glasses inserted in a 24-multiwell plate. After 8 days of differentiation, the samples were characterized using the protocol of immunofluorescence staining of β-tubulin III co-labeling the nuclei with DAPI as described in Chelli et al.[39]

Conclusions

We developed a novel composite material able to host RA. In combination with fibrin gel, it induced proliferation and differentiation of stem cells. Fibrin acts as a fully bioresorbable 3D scaffold where cells adhere and migrate and whose degradation can be tuned using proper enzyme inhibitors. The incorporated RA can be released in an acidic environment, such as that in proximity of the chosen cell lines. Differentiation of both embryonic neuroectodermal stem cells and secondary neuroblastoma cells towards neuronal cells has been achieved and cells formed a three-dimensional neuronal network in the environment provided by the composite scaffold. Our results pose the bases for the fabrication of implantable scaffold as new active coating of implantable devices both to prevent nosocomial infections,[ii] and to promote integration in the hosting organism.[40]

Conflicts of interest

There are no conflicts to declare.

Author Contributions

Conceived and designed the experiments: GF, MC, FZ, GP, FB, MB and FV. Performed the Imaging experiments: MB, FV, MDG, GF, GM; performed the cell differentiation experiments: MB, MDG, GM; Analyzed the data: GF, BP, IP, FV, SF, FB, GM and FZ; performed the diffraction data: IP, BP; synthesis of the composite materials: MDG, MB, GM; kinetic of release experiments: GM and MDG. Wrote the paper: All the co-authors. Gave conceptual advice: All the co-authors.

Acknowledgements

The authors would like to thank the SPM@ISMN facility for the support in collecting microscopy images. This work was partially supported by EU NMP Project Grant Agreement n. 280772 iONE-FP7 and Italian flagship NANOMAX project N-CHEM.

References

1. H. E. Davis and J. K. Leach, *Ann Biomed Eng*, 2011, **39**, 1-13.
2. B. C. Thompson, S. E. Moulton, J. Ding, R. Richardson, A. Cameron, S. O'Leary, G. G. Wallace and G. M. Clark, *J Control Release*, 2006, **116**, 285-294.
3. A. L. Berman A., Weiner S *Nature*, 1988, **331**, 546-548.
4. R. A. Metzler, G. A. Tribello, M. Parrinello and P. U. Gilbert, *J Am Chem Soc*, 2010, **132**, 11585-11591.
5. B. A. Gotliv, N. Kessler, J. L. Sumerel, D. E. Morse, N. Tuross, L. Addadi and S. Weiner, *Chembiochem*, 2005, **6**, 304-314.
6. F. Nudelman, B. A. Gotliv, L. Addadi and S. Weiner, *J Struct Biol*, 2006, **153**, 176-187.
7. F. Nudelman and N. Sommerdijk, *Angew. Chem.-Int. Edit.*, 2012, **51**, 6582-6596.
8. B. Pokroy, A. N. Fitch, P. L. Lee, J. P. Quintana, E. N. Caspi and E. Zolotoyabko, *Journal of Structural Biology*, 2006, **153**, 145-150.
9. E. Weber and B. Pokroy, *CrystEngComm*, 2015, **17**, 5873-5883.
10. F. C. Meldrum, *Int. Mater. Rev.*, 2003, **48**, 187-224.
11. F. C. Meldrum and H. Colfen, *Chem. Rev.*, 2008, **108**, 4332-4432.
12. A. Brif, G. Ankonina, C. Drathen and B. Pokroy, *Adv Mater*, 2014, **26**, 477-481.
13. G. Magnabosco, M. Di Giosia, I. Polishchuk, E. Weber, S. Fermani, A. Bottoni, F. Zerbetto, P. G. Pelicci, B. Pokroy, S. Rapino, G. Falini and M. Calvaresi, *Adv. Healthc. Mater.*, 2015, **4**, 1510-1516.
14. Y. Y. Kim, A. S. Schenk, D. Walsh, A. N. Kulak, O. Cespedes and F. C. Meldrum, *Nanoscale*, 2014, **6**, 852-859.
15. A. N. Kulak, P. C. Yang, Y. Y. Kim, S. P. Armes and F. C. Meldrum, *Chem. Commun.*, 2014, **50**, 67-69.
16. D. C. Green, J. Ihli, P. D. Thornton, M. A. Holden, B. Marzec, Y. Y. Kim, A. N. Kulak, M. A. Levenstein, C. Tang, C. Lynch, S. E. D. Webb, C. J. Tynan and F. C. Meldrum, *Nat. Commun.*, 2016, **7**, 13.
17. C. Besson, E. E. Finney and R. G. Finke, *Chemistry of Materials*, 2005, **17**, 4925-4938.
18. K. R. Cho, Y. Y. Kim, P. C. Yang, W. Cai, H. H. Pan, A. N. Kulak, J. L. Lau, P. Kulshreshtha, S. P. Armes, F. C. Meldrum and J. J. De Yoreo, *Nat. Commun.*, 2016, **7**, 7.
19. Y. Y. Kim, K. Ganesan, P. C. Yang, A. N. Kulak, S. Borukhin, S. Pechook, L. Ribeiro, R. Kroger, S. J. Eichhorn, S. P. Armes, B. Pokroy and F. C. Meldrum, *Nat. Mater.*, 2011, **10**, 890-896.
20. Y. Y. Kim, M. Semsarilar, J. D. Carloni, K. R. Cho, A. N. Kulak, I. Polishchuk, C. T. Hendley, P. J. M. Smeets, L. A. Fielding, B. Pokroy, C. C. Tang, L. A. Estroff, S. P. Baker, S. P. Armes and F. C. Meldrum, *Adv. Funct. Mater.*, 2016, **26**, 1382-1392.
21. J. W. C. Dunlop and P. Fratzl, *Annual Review of Materials Research*, 2010, **40**, 1-24.
22. S. Borukhin, L. Bloch, T. Radlauer, A. H. Hill, A. N. Fitch and B. Pokroy, *Adv. Funct. Mater.*, 2012, **22**, 4216-4224.
23. A. E. X. Brown, R. I. Litvinov, D. E. Discher, P. K. Purohit and J. W. Weisel, *Science*, 2009, **325**, 741-744.
24. L. Altucci and H. Gronemeyer, *Trends in Endocrinology & Metabolism*, 2001, **12**, 460-468.
25. M. B. Soderlund, A. Sjoberg, G. Svard, G. Fex and P. Nilsson-Ehle, *Scand. J. Clin. Lab. Invest.*, 2002, **62**, 511-519.
26. T. A. E. Ahmed, E. V. Dare and M. Hincke, *Tissue Eng. Part B-Rev.*, 2008, **14**, 199-215.
27. D. M. Albala, *Cardiovasc. Surg.*, 2003, **11**, 5-11.
28. T. Fattahi, M. Mohan and G. T. Caldwell, *J. Oral Maxillofac. Surg.*, 2004, **62**, 218-224.
29. M. R. Jackson, *Am. J. Surg.*, 2001, **182**, 1S-7S.
30. N. Laurens, P. Koolwijk and M. P. M. De Maat, *J. Thromb. Haemost.*, 2006, **4**, 932-939.
31. G. Pellegrini, P. Rama, F. Mavilio and M. De Luca, *J. Pathol.*, 2009, **217**, 217-228.
32. Q. Ye, G. Zund, P. Benedikt, S. Jockenhoevel, S. P. Hoerstrup, S. Sakyama, J. A. Hubbell and M. Turina, *Eur. J. Cardio-Thorac. Surg.*, 2000, **17**, 587-591.
33. Y. Kato, S. Ozawa, C. Miyamoto, Y. Maehata, A. Suzuki, T. Maeda and Y. Baba, *Cancer Cell Int.*, 2013, **13**, 8.

34. B. Pokroy, A. N. Fitch and E. Zolotoyabko, *Adv. Mater.*, 2006, **18**, 2363-+.
35. R. M. Zachariah, C. O. Olson, C. Ezeonwuka and M. Rastegar, *PLoS One*, 2012, **7**, 10.
36. M. Barbalinardo, D. Gentili, F. Lazzarotto, F. Valle, M. Brucale, M. Melucci, L. Favaretto, M. Zambianchi, A. I. Borrachero-Conejo, E. Saracino, V. Benfenati, D. Natalini, P. Greco, M. G. Di Carlo, G. Foschi and M. Cavallini, *Small Methods*, 2018, **2**.
37. T. Posati, A. Pistone, E. Saracino, F. Formaggio, M. G. Mola, E. Troni, A. Sagnella, M. Nocchetti, M. Barbalinardo, F. Valle, S. Bonetti, M. Caprini, G. P. Nicchia, R. Zamboni, M. Muccini and V. Benfenati, *Sci Rep*, 2016, **6**, 16.
38. T. Cramer, B. Chelli, M. Murgia, M. Barbalinardo, E. Bystrenova, D. M. de Leeuw and F. Biscarini, *Phys. Chem. Chem. Phys.*, 2013, **15**, 3897-3905.
39. B. Chelli, M. Barbalinardo, F. Valle, P. Greco, E. Bystrenova, M. Bianchi and F. Biscarini, *Interface Focus*, 2014, **4**.
40. S. B. Goodman, Z. Y. Yao, M. Keeney and F. Yang, *Biomaterials*, 2013, **34**, 3174-3183.